ACS OMEGA

http://pubs.acs.org/journal/acsodf

Article

Biosensors Based on Acetylcholinesterase Immobilized on Clay−Gold Nanocomposites for the Discrimination of Chlorpyrifos and Carbaryl

Angkana Phongphut, Bralee Chayasombat, Anthony E. G. Cass, Muenduen Phisalaphong, Seeroong Prichanont, Chanchana Thanachayanont, and Thanawee Chodjarusawad*

Cite This: *ACS Omega* 2022, 7, 39848−39859

Read Online

ACCESS | Metrics & More | Article Recommendations | Supporting Information

ABSTRACT: This work aims at evaluating a utilization of diverse clay mineral/gold nanoparticles/acetylcholinesterase (clay/AuNPs/AChE) biosensors by using principal component analysis (PCA) for the discrimination of pesticide types and their concentration levels both in the synthetic and real samples. Applications of simple and low-cost clay/AuNP composites of different characteristics as modified-electrode materials are highlighted. Four types of clay minerals, namely, platelike kaolinite (Kaol: 1:1 aluminum phyllosilicate), globular montmorillonite (Mt: 2:1 aluminum phyllosilicate), globular bentonite (Bent: 2:1 aluminum phyllosilicate), and fibrous sepiolite (Sep: 2:1 inverted ribbons of magnesium phyllosilicate), were selected as the base materials. Due to the distinct characteristics of the selected clay, the derived clay/AuNP composites resulted in different physical morphologies, AuNP sizes and loadings, matrix hydrophobicity, and active AChE loading per electrode. These, in turn, caused divergent electrochemical responses for the pesticide determination; hence, no other enzymes apart from AChE were necessary for the fabrication of distinct biosensors. Physical and chemical characterizations of clay/AuNPs were conducted using scanning electron microscopy, transmission electron microscopy, thermogravimetric analysis, and X-ray photoelectron spectroscopy techniques. The electrochemical information was recorded by cyclic voltammetry and amperometry techniques. The enzyme inhibition results obtained from the pesticides were treated and used as input data to obtain PCA results. The four fabricated clay/AuNPs/AChE biosensors were able to discriminate chlorpyrifos and carbaryl and their concentration levels for synthetic pesticides and real samples. It was disclosed that a high enzyme inhibition and a high hydrophobic modified-electrode material affect a highly sensitive pesticide biosensor. The hydrophobic/hydrophilic character of the modified-electrode material plays a major role in discriminating the pesticide types and their concentration levels by the proposed single-enzyme sensor system. The PCA results illustrated that PC2 described the different types of pesticides, and PC1 showed the level of pesticide concentration with high first two principal components. The mixed pesticides could be identified at an especially low total concentration of 0.5 ng/mL in real samples.

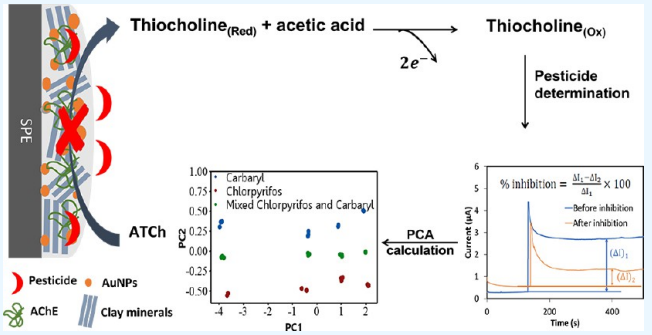

1. INTRODUCTION

Organophosphates and carbamates (OPs and CMs) are widely used in agriculture for insecticidal activities. Unfortunately, pesticide residues that are present in foods and contaminated drinking water are toxic to human health due to their inhibitory effect on acetylcholinesterase (AChE) which causes neurodegenerative diseases such as Parkinson's, Alzheimer's disease, schizophrenia, and epilepsy.[1−3] Maximum residue levels (MRLs) are, therefore, set by the national and international authorities to control levels of pesticide residues in food. In this regard, the identification and quantification of pesticide residues are crucial. The conventional methods used for pesticide determination are based on mass spectrometry, such as gas chromatography and liquid chromatography, which are of great precision. However, these techniques require tedious extraction, expensive reagents, time-consuming sample pretreatment, expensive equipment, and professional technicians to analyze.[4] Hence, biosensors based on AChE inhibition have attracted vast interest because of their simple preparation procedures, fast responses, excellent sensitivity, and on-site field portability.[5−8]

To date, various AChE biosensors have been developed applying different techniques for pesticide determination, such as the electrochemical method,[1,4,9] spectrophotometric sens-

Received: June 22, 2022
Accepted: October 14, 2022
Published: October 26, 2022

ing,[10] optical method,[11−13] and microcantilever.[14] Nonetheless, the determination of mixed OPs and/or CMs by an AChE biosensor of any technique can only be displayed in one cumulative value. The final outcome of the AChE biosensor, hence, depends on varied attribution of each pesticide on the enzyme inhibition. As a result, the specific types of pesticides and their corresponding concentrations in mixed-pesticide solutions cannot be identified using a single AChE biosensor.

To identify types of pesticides and their corresponding concentration levels, attempts have been made to combine analytical responses from distinctive biosensors with mathematical interpretation using principal component analysis (PCA).[15,16] One popular method to achieve diverse biosensors is to fabricate each sensor with a different enzyme. For example, AChE, butyrylcholinesterase (BChE), tyrosinase, horseradish peroxidase, soybean peroxidase, cellobiose dehydrogenase, and glucose oxidase were incorporated in a biosensor array for the amperometric analysis of wastewater samples in conjunction with PCA.[17−19] Chemical oxygen demand, total organic carbon, and biochemical oxygen demand were discriminated. However, none of the pesticides and their concentration levels were identified. Moreover, AChE and choline oxidase were applied in combination with PCA for the analyses of Ops (chlorpyrifos, dimethoate, methamidophos, phoxim, and triazophos), CMs (bicarb, carbaryl, isoprocarb, methomyl, and metolcarb), and other pesticides using a colorimetric biosensor array.[20] Different classes (not types) of pesticides could be discriminated at a tested concentration of 10 ng/mL. Recently, a multichannel fluorescent array system consisting of three cholinesterases (AChEs from electric eels and head of the fly and BChE from equine serum) has been applied together with PCA to classify 30 Ops and CMs into pesticides of high and low toxicity to the lowest concentration of 0.2 μg/mL.[21] All reports have demonstrated that different enzyme biosensors and PCA are powerful tools for the determination of organic pollution parameters or pesticide types and their corresponding concentration levels. Despite the satisfactory results, the uses of a system with various enzymes are costly and complicated in some issues, such as different measuring and storage conditions and varied shelf lives.

The other widely acknowledged method for the fabrication of a system with diverse sensors for pesticide determination is the nonenzyme technique. Various "smart materials," such as nanocomposites, have been synthesized and modified on a conventional substrate to obtain disparate response signals useful for PCA. Examples are the sensor arrays of interdigitated electrodes modified with reduced graphene oxide (rGO), polypyrrole/reduced graphene oxide (PPy/rGO), poly(3,4-ethylene dioxythiophene):poly(styrenesulfonate)/reduced graphene oxide (PEDOT:PSS/rGO), and poly(3,4-ethylene dioxythiophene):poly(styrenesulfonate)/reduced graphene oxide/gold nanoparticles (PEDOT:PSS-rGO-AuNPs) to detect and discriminate mixtures of Ops (malathion and cadusafos) in real samples by an impedimetric electronic tongue.[15] These sensor arrays were able to classify different pesticides at nanomolar concentrations using the materials with different electrochemical responses. A chlorpyrifos gas sensor was developed by self-assembled nanoparticle networks and four different polymer coatings, namely, poly(ethyl methacrylate), poly(2-hydroxyethyl methacrylate), poly(isobutyl methacrylate), and poly(butyl methacrylate).[22] The sensors were ultimately able to distinguish between chlorpyrifos and its solvent, detecting 0.7 ng/mL in the gas phase. Chemiluminescent sensors incorporating the luminol and silver nanoparticles (Lum-AgNP) for the detection of five OPs and CMs, including dimethoate, dipterex, carbaryl, chlorpyrifos, and carbofuran, have been distinguished at a concentration of 24 μg/mL.[23] Moreover, gold and silver nanoparticles were doped with L-arginine, quercetin, and polyglutamic acid to discriminate carbaryl, paraoxon, parathion, malathion, diazinon, and chlorpyrifos using a colorimetric method.[24] These sensors can determine the individual pesticides at 22.0−36.0 ng/mL. All reports revealed crucial information that modified-substrate materials with distinct characteristics resulted in unique sensor responses in the presence of mixed pesticides. These signals, when combined with PCA, derive a powerful tool for identifying pesticide types and their concentration levels. Unfortunately, most "smart materials" require fine raw materials and precisely controlled synthetic conditions and are expensive.

Clay minerals, of low cost and naturally abundant, have been proven as excellent supports for enzyme immobilization resulting in enhancement of enzyme activity and stability.[25−27] The materials can be classified into three unique layer-silicates[28] demonstrating their diverse characteristics. Our previous work[27] revealed that different clay/gold nanoparticles (clay/AuNPs) resulted in distinct effects on AChE loading, activities, stability, and, finally, the capability for chlorpyrifos detection. Therefore, we postulated that the cheap and simple clay/AuNPs of different categories could be applied to construct diverse biosensors based only on a single AChE for mixed pesticide detection. Thus, complications due to the use of different types of enzymes and the need to synthesize "smart materials" can be eliminated. The obtained response signals when analyzed in combination with PCA were predicted to be capable of discriminating types of pesticides and their concentration levels.

The ultimate aim of this work is, therefore, to evaluate the potential application of different clay/AuNPs/AChE biosensors using the amperometric technique in conjunction with PCA for discriminating chlorpyrifos from carbaryl at different concentration levels in mixed pesticide solutions. Four types of clay minerals, namely, platelike kaolinite (Kaol), globular montmorillonite (Mt), globular bentonite (Bent), and fibrous sepiolite (Sep), were selected as the base materials for sensor fabrication. Physical, chemical, and electrochemical characteristics of the four clay/AuNPs composites were analyzed to shed light on the different sensor behaviors. In addition, suitable operating conditions for pesticide detection were assessed for each biosensor on the synthetic pesticide and additional standard pesticide on real samples. Finally, PCA analyses of response signals from the four biosensors were demonstrated for individual chlorpyrifos and carbaryl and their mixed solutions. To the best of our knowledge, this article demonstrates types of pesticides and their concentration levels can be distinguished using only a single AChE on diverse and extremely cheap clay mineral-based sensors.

2. EXPERIMENTAL SECTION

2.1. Chemicals and Reagents. Acetylcholinesterase (AChE, EC 3.1.1.7, Type VI-S, 254 U/mg from electric eels), acetylthiocholine chloride (ATCh), chlorpyrifos, carbaryl, kaolinite (Kaol), montmorillonite (Mt), bentonite (Bent), sepiolite (Sep), hydrogen tetrachloroaurate ($HAuCl_4 \cdot 3H_2O$), sodium borohydride ($NaBH_4$), 3-aminopropyl triethoxysilane (APTES), 5,5′-dithiobis(2-nitrobenzoic acid) (DTNB), diso-

https://doi.org/10.1021/acsomega.2c03899
ACS Omega 2022, 7, 39848−39859

dium hydrogen phosphate (Na_2HPO_4), sodium dihydrogen phosphate (NaH_2PO_4), sodium hydroxide (NaOH), potassium chloride (KCl), and potassium ferricyanide ($K_3[Fe(CN)_6]$) were purchased from Sigma-Aldrich. In addition, 100% acetic acid (CH_3COOH) and 99.9% ethanol (CH_3CH_2OH) were obtained from QReC Chemical. Chitosan (CS, average M_W = 550 kDa, and 95% acetylation) was obtained from Seafresh Chitosan Co., Ltd., Thailand. Deionized water was prepared from a Thermo Scientific Barnstead EASY pure deionization unit. All the chemicals used were of analytical grade and applied without further treatment.

2.2. Apparatus. Physical and chemical characterizations of the materials were achieved using the following equipment: a UV-2450 spectrophotometer (Shimadzu Co., Japan) for UV−vis absorption spectroscopy, a scanning electron microscope (SEM; JEOL JSM-5410, Japan), and a transmission electron microscope (TEM, JEOL JEM-2010). The amount of gold loading was tested by X-ray photoelectron spectroscopy (XPS; Kratos AXIS Supra), while the weight of adsorbed water was evaluated using a thermogravimetric analyzer (TGA; PerkinElmer TGA 7).

The electrochemical measurements of cyclic voltammetry (CV) and amperometry were performed with an Autolab potentiostat (Metrohm, model PGSTAT101) with Nova software version 1.11. A conventional three-electrode system was used with a screen-printed carbon electrode (SPE) from Quasense Co., Ltd. (Thailand) as the working electrode, a silver/silver chloride reference electrode (Ag/AgCl, saturated KCl), and a platinum counter electrode from Metrohm.

2.3. Synthesis of Clay/AuNPs. To modify AuNPs on the surface of clay minerals, the pristine clay minerals were primarily grafted with APTES, which acted as anchors for the gold precursor. To achieve this, 1.5 mL of APTES was added to a 20 mL ethanol solution in a Teflon bottle and kept under stirring for 5 min at room temperature. Then, 1.2 g of the selected clay mineral was added to the prepared solution, which was stirred for another 30 min. Subsequently, the mixture was oven-heated to 85 °C and held at this temperature for 24 h. The achieved material was next filtered using a Whatman No. 5 paper and washed once using a 100 mL ethanol solution. The recovered product (clay/APTES) was then dried at 80 °C for 12 h.[29] To attach the gold precursor, 1 g of the dried clay/APTES was continuously stirred in a 0.5 mM gold precursor (50 mL) solution for 3 h before being filtered and washed with distilled water. Then, the clay/APTES/Au^{3+} was dried at 80 °C for 12 h. The reduction of Au(III) was next performed by adding 1 mL of a 0.1 M $NaBH_4$ aqueous solution to 50 mg of the dried clay/APTES/Au^{3+} and kept stirring at room temperature for 10 min. The obtained particles were consecutively filtered, washed with a large amount of distilled water, and air-dried. The red wine clay/AuNPs was finally achieved.

2.4. Preparation of the AChE Biosensor. To immobilize AChE onto the surface of clay/AuNPs (Kaol/AuNPs, Mt/AuNPs, Bent/AuNPs, and Sep/AuNPs), 0.001 g of AChE was first dissolved under mild stirring in 2 mL of 0.1 M PBS (pH 6.0) at 4 °C for 10 min. Then, 0.1 g of the clay/AuNPs was added to the AChE solution and stirred for another 2 h at 4 °C. The suspension was consequently filtered with Whatman No. 5 paper and washed with 2 mL of 0.1 M PBS (pH 6.0) to remove the unbound AChE. Finally, the retained 0.1 g of clay/AuNPs/AChE (denoted as Kaol/AuNPs/AChE, Mt/AuNPs/AChE, Bent/AuNPs/AChE, and Sep/AuNPs/AChE) was redispersed in 2 mL of 0.1 M PBS (pH 6.0). Later, 3 μL of the clay/AuNPs/AChE was drop-cast onto the SPE surface (0.06 cm^2 active area) and air-dried at room temperature. Then, 3 μL of a chitosan solution (0.5% w/v, pH 6.0) was coated on the modified SPE and allowed to dry in a desiccator for 10 min. After drying, the modified electrodes, namely, SPE/Kaol/AuNPs/AChE/CS, SPE/Mt/AuNPs/AChE/CS, SPE/Bent/AuNPs/AChE/CS, and SPE/Sep/AuNPs/AChE/CS biosensors, were obtained. All electrodes were freshly prepared and used within the day of the experiments.

2.5. Enzyme Loading and Enzyme Residual Activity Active Enzyme per Electrode. Active enzyme per electrode was determined using the amount of enzyme loading and the residual activity of immobilized AChE and calculated using eq 1. The amount of the enzyme per electrode was measured with a spectrophotometer at 277 nm and calculated using eq 2, where E_{in} and E_{un} are the amount of initial enzyme and the amount of unbound enzyme, respectively. The residual enzyme activity was determined using Ellman's method.[30] The hydrolyzed product, thiocholine, reacted with the added DTNB and resulted in a yellowish product. The color intensity of the product was measured at 412 nm and proportional to the enzyme activity. An enzyme solution, 20 μL of 100 mM ATCh, 3 mL of 0.1 M PBS (pH 6.0), and 100 μL of 10 mM DTNB were mixed and reacted for 2 min. Then, the solution was suddenly measured using a spectrophotometer at 412 nm, and the residual enzyme activity was calculated using eq 3. A_{im} and A_{free} represent the absorbance from Ellman's reaction of the immobilized enzyme and fresh free enzyme.

$$\text{Active enzyme} = [\text{amount of enzyme per electrode} \times \text{enzyme residual activity (\%)}]/100 \quad (1)$$

$$\text{amount of enzyme per electrode} = (E_{in} - E_{un})/E_{in} \quad (2)$$

$$\text{enzyme residual activity (\%)} = (A_{in}/A_{free}) \times 100 \quad (3)$$

2.6. Electrochemical Measurements. The CVs were tested in 0.1 M PBS (pH 9.0) in the presence of 10 mM $[Fe(CN)_6]^{3-/4-}$ containing 0.1 M KCl and 0.1 M PBS containing 10 mM ATCh. For pesticide determination, the fabricated AChE biosensors were employed for the determination of pesticides using an amperometric method. First, the initial response of the biosensor was tested in a 0.1 M PBS solution containing ATCh at the specified concentration. Then, the electrode was rinsed once with the 0.1 M PBS solution (pH 9.0) and incubated in a pesticide solution (chlorpyrifos and/or carbaryl) for a certain period of time. Finally, the electrode was then tested in the same ATCh solution for the second amperometric measurement. The inhibition percentage of AChE by the pesticide was calculated as follows:

$$\text{inhibition (\%)} = [(\Delta I_1 - \Delta I_2)/\Delta I_1] \times 100 \quad (4)$$

where ΔI_1 and ΔI_2 represent the current responses, respectively, before and after the incubation procedure. The limit of detection (LOD) was determined according to the following equation:

$$\text{LOD} = 3S_b/m \quad (5)$$

where S_b refers to the standard deviation of the blank, and m represents the slope of the calibration curve.

https://doi.org/10.1021/acsomega.2c03899
ACS Omega 2022, 7, 39848−39859

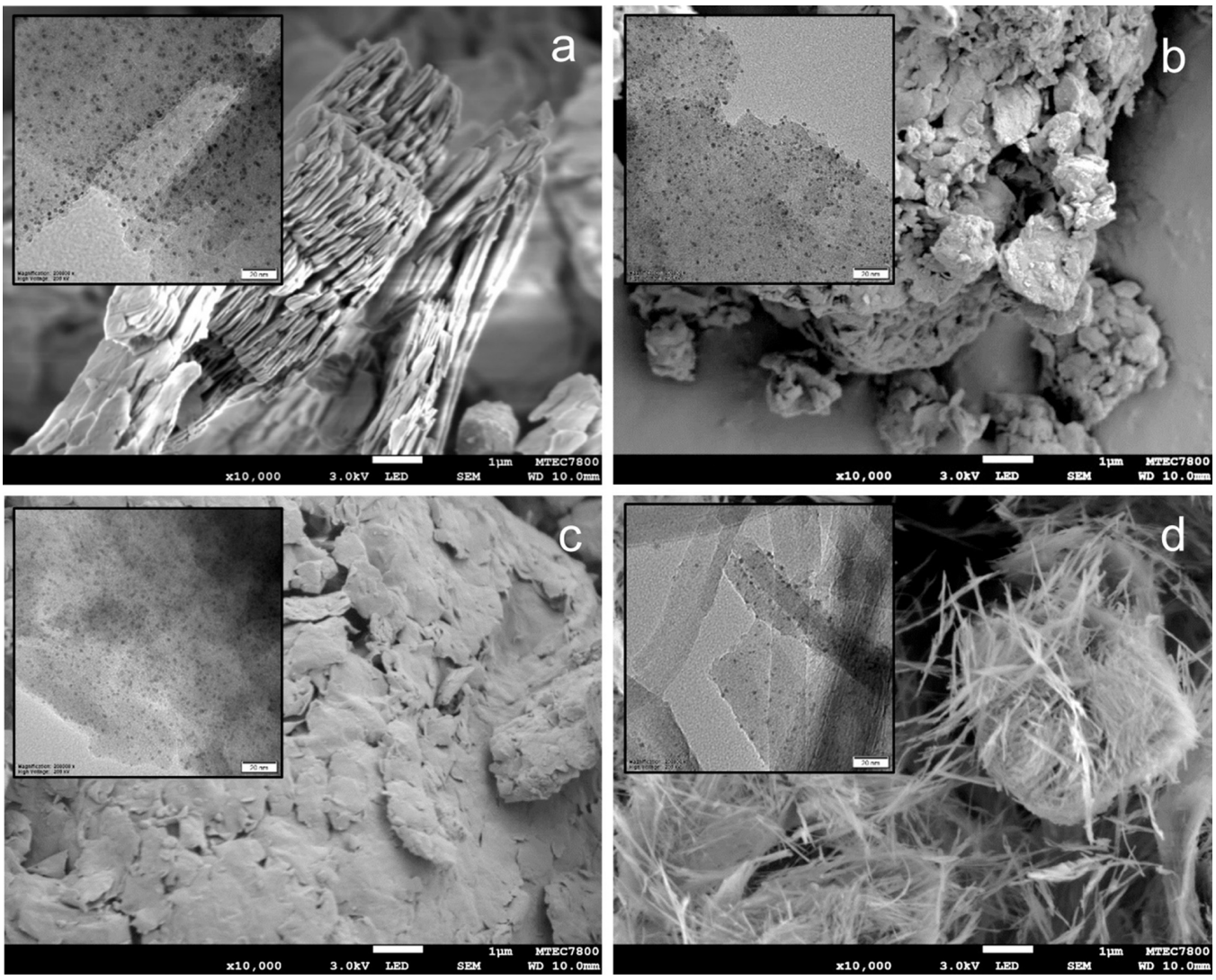

Figure 1. SEM images of pristine clay minerals and TEM images of AuNP-decorated clay minerals (inset); (a) Kaol, (b) Mt, (c) Bent, and (d) Sep.

2.7. Preparation for Pesticide Analyses in Real Samples. To analyze pesticides in real samples (using carrots as a representative), a previously reported method[31] was used for the preparation of carrot juice. Briefly, 5 g of carrots obtained from a local market were chopped into cubes of 0.5 cm and were put in the test tube containing 10 mL of 5% ethanol. The samples were then hand-shaken for 1 min and incubated at room temperature for another 10 min. Next, the carrot juice was separated from the solid matrix using filtration paper. Finally, the specified pesticide was injected to the prepared juice at the described concentration, and the electrochemical experiment was followed.

2.8. Data Treatment. To discriminate the pesticide types and concentration levels, the pesticide inhibitions obtained from the alternate biosensors were treated by a PCA using commercial software minitab19. Prior to the PCA, the pesticide inhibition data were preprocessed according to the following equations:

$$\text{data set} = \log[\%\text{inhibition}]/\text{slope} \quad (6)$$

$$\text{slope} = \text{delta}(\log[\%\text{inhibition}])/\text{delta}(\log[\text{pesticide concentration}]) \quad (7)$$

The pesticide inhibition was arranged into a data set matrix with the selected response variables defining the columns (pesticide concentration) and the rows (data set from eq 6) referring to the sample measurements. When the data set matrix was distinguished by PCA, new axes were created, such that PC1 described the largest variance in the data and PC2 the second-largest amount of data variance constructed orthogonal to PC1 and independent on PC1.

3. RESULTS AND DISCUSSION

3.1. Physical and Chemical Characterization. Four different kinds of clay/AuNPs were collectively applied as modified-electrode materials for the immobilization of AChE from the same source to determine the types of pesticides and their concentration levels. The proposed biosensors were tested in model solutions containing chlorpyrifos and/or carbaryl. Since the only alteration of the four studied electrodes was the types of modifying materials, the characterization of these materials was essential. The surface morphology of pristine clay minerals was observed by scanning electron microscopy (SEM), as presented in Figure 1. Kaol (Figure 1a) shows pseudo-hexagonal platelike and booklet agglomerates,[32,33] while Mt (Figure 1b) and Bent (Figure 1c) are in

https://doi.org/10.1021/acsomega.2c03899
ACS Omega 2022, 7, 39848−39859

aggregated and coarse morphology.[34,35] In contrast, Sep (Figure 1d) portrays a fibrous characteristic, which can aggregate into bundles.[36,37] Decoration of the clay minerals with gold nanoparticles (clay/AuNPs) was achieved primarily by grafting APTES on the clay surfaces (clay/APTES), followed by adsorption and reduction of the gold precursors. The dark spots in the TEM images (insets of Figure 1) show well-dispersed gold nanoparticles on the clay structures. The average diameters of the AuNPs on Kaol, Mt, Bent, and Sep are 2.98 ± 0.43 nm (n = 250), 1.99 ± 0.38 nm (n = 250), 2.18 ± 0.50 (n = 250), and 2.16 ± 0.63 nm (n = 250), respectively. Further, the clay/AuNPs were characterized by XPS. The XPS signals at the high resolution of the clay/AuNPs (Figure S1) show the Au4f spectrum indicating the presence of Au atoms.[38] The amounts of gold loading from XPS are in the following order: Kaol/AuNPs > Bent/AuNPs > Mt/AuNPs > Sep/AuNPs (Table 1). Besides, the order of the hydrophobicity of the modified-electrode materials is Kaol/AuNPs > Mt/AuNPs > Bent/AuNPs > Sep/AuNPs (see Table 1). This interpretation was based on the amounts of adsorbed water on the surface of clay/AuNPs by TGA, as shown in Figure S2.

Table 1. Characteristics of the Fabricated Clay/AuNPs/AChE Biosensors[a]

types of clay	AuNP loading (wt %)	weight of adsorbed water on the surface (wt %)	active unit of AChE per electrode	current response (μA)
Kaol/AuNPs	3.11	0	0.129	15.02 ± 0.83[a]
Mt/AuNPs	1.62	3.34	0.212	21.89 ± 0.39[b]
Bent/AuNPs	2.17	3.56	0.176	18.86 ± 0.56[c]
Sep/AuNPs	0.96	7.53	0.137	15.94 ± 0.29[a]

[a]Statistical analysis results show that values of the same letter (a, b, c) within the same column are not significantly different and vice versa for values of different letters within the same column, judged from the Fisher LSD method and 95% confidence intervals for each pair of parameters.

3.2. Electrochemical Behavior of the Clay/AuNP Nanocomposites. In order to investigate the electrochemical properties of the bare SPE, SPE/clay/CS, and SPE/clay/AuNPs/CS electrodes, CV was performed in a 10 mM $[Fe(CN)_6]^{3-/4-}$ solution containing 0.1 M KCl as shown in Figure 2. Modification of the bare SPE with pristine clays (red line) resulted in the lowest oxidation and reduction peak currents in all cases. This was presumably due to the hindrances of the negatively charged clays to the negative charge $[Fe(CN)_6]^{3-/4-}$.[39] In addition, the poor conductivity of pristine clays[27] derived the higher charge-transfer resistances of SPE/clay/CS in comparison to the bare SPE. However, the inclusion of the AuNPs on the pristine clays lowered the negativity of the matrix charge[27] and strikingly promoted the electron transfer between the working electrode and solution redox species. Thus, the upsurge in peak currents and reduction of the peak-to-peak potential separation (ΔE_p) is observed.[40] Interestingly, the decrease in ΔE_p is linearly proportional to the amounts of incorporated AuNPs regardless of the particle sizes (Figure 3a). This indicates an influential effect of AuNPs on electrode performance. Furthermore, not only integrated AuNPs were found governing the sensor performances but also the hydrophobic/hydrophilic nature of the modified-electrode materials. Figure 3b interestingly shows linear relations between amounts of adsorbed water on the clay/AuNPs and the obtained peak currents. The increased hydrophilicity of clay/AuNPs is likely due to concentrated $Fe(CN)_6^{3-/4-}$ in the material matrix, hence enhancing the diffusion rate of the solute.

To identify the electrode mechanism, the SPE/clay/CS and SPE/clay/AuNPs/CS electrodes were tested under varied scan rates in solutions containing 10 mM $[Fe(CN)_6]^{3-/4-}$ and 0.1 M KCl (Figures S3 and S4). The insets in Figures S3 and S4 demonstrate that the anodic and cathodic peak currents are proportional to the square root of the scan rate in all cases. This result indicates a typical diffusion-controlled reaction in agreement with the Randles−Sevcik equation as follows:[41]

$$i_p = 2.69 \times 10^5 D^{1/2} n^{3/2} C A \upsilon^{1/2} \quad (8)$$

where i_p is the peak current (amps), A is an electroactive surface area (cm^2), D is the diffusion coefficient of the analyte (cm^2/s), n is the number of transferred electrons, C is the concentration of the redox molecules in a solution (mol/cm^3), and υ is the scan rate (V/s). The electroactive surface areas of the bare SPE, SPE/Kaol/CS, SPE/Mt/CS, SPE/Bent/CS, and SPE/Sep/CS were calculated at 0.016, 0.017, 0.016, 0.016, and 0.017 cm^2, respectively. Similarly, the electroactive surface areas of the SPE/clay/AuNPs/CS electrodes were determined at 0.018, 0.023, 0.024, and 0.028 cm^2 for SPE/Kaol/AuNPs/CS, SPE/Mt/AuNPs/CS, SPE/Bent/AuNPs/CS, and SPE/Sep/AuNPs/CS, respectively. It is evident that pristine clays hardly enhanced SPE electroactive surface area. In contrast, modification of the SPE electrodes with clay/AuNPs considerably resulted in higher electroactive surface areas, up to 70.5% for the case of Sep. Surprisingly, the designated order of electroactive surface areas for clay/AuNPs corresponded to the hydrophilicity of the composites: Sep/AuNPs > Bent/AuNPs > Mt/AuNPs > Kaol/AuNPs. There is potentially a correlation between the electroactive surface area and the hydrophobic/hydrophilic nature of the matrix. Since the solute is highly hydrophilic, the hydrophilic surface is thus portrayed as the electroactive surface area.

To summarize, it is demonstrated here that the SPE/clay/CS and SPE/clay/AuNPs/CS electrodes resulted in the diffusion-control reaction for the $[Fe(CN)_6]^{3-/4-}$ redox couple. Incorporated AuNPs and the hydrophobic/hydrophilic character of the clay/AuNP composites play governing roles in the sensor performances. First, the inclusion of AuNPs to the pristine clays tremendously enhances electron transfer between the solute and the electrode surface, resulting in the upsurge of peak currents and the lowered peak-to-peak separation. Second, the reduction in peak-to-peak separation was evidently proportional to the amounts of AuNP loading in the selected clays regardless of the AuNP sizes. Finally, the hydrophobic/hydrophilic nature of the electrode-modified materials closely affects the solute accumulation in the matrix and its diffusion rate, which influences the electroactive surface area and the current response.

3.3. SPE/Clay/AuNPs/AChE/CS Biosensors and Their Electrochemical Behaviors. To fabricate a biosensor for pesticide detection, AChE from the same source was immobilized on the clay/AuNPs modified-electrode materials before being covered by the chitosan film (CS) and denoted as SPE/clay/AuNPs/AChE/CS. Two reactions are involved in the process. First, ATCh is hydrolyzed to thiocholine and

https://doi.org/10.1021/acsomega.2c03899
ACS Omega 2022, 7, 39848−39859

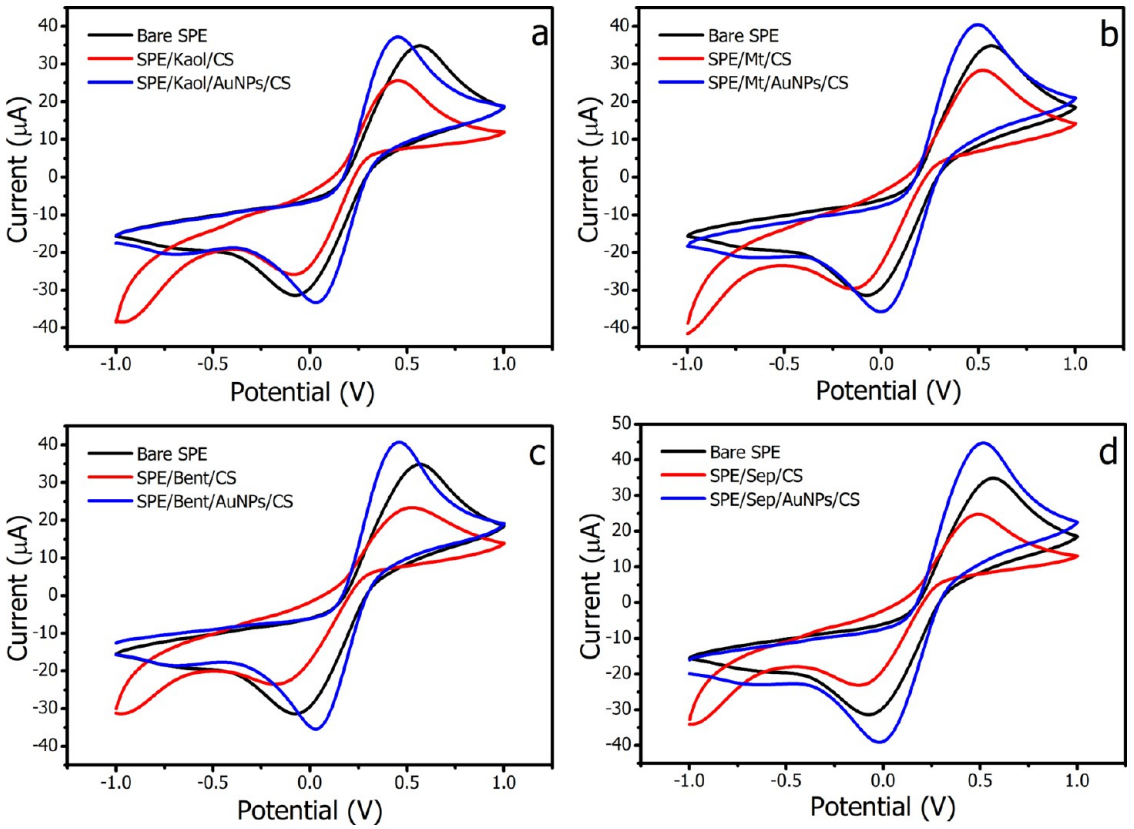

Figure 2. Cyclic voltammograms of bare SPE, SPE/clay/CS, and SPE/clay/AuNPs/CS: (a) Kaol, (b) Mt, (c) Bent, and (d) Sep in 0.1 M PBS (pH 9.0) containing 10 mM $[Fe(CN)_6]^{3-/4-}$ and 0.1 M KCl; scan rate 50 mV/s.

acetic acid by AChE (eq 9), and second, thiocholine is oxidized to dithio-bis-choline on the electrode surface according to eq 10.

$$\text{acetythiocholine} + H_2O \xrightarrow{\text{AChE}} \text{thiocholine} + \text{acetic acid} \quad (9)$$

$$2\text{thiocholine} \rightarrow \text{dithio} - \text{bis} - \text{choline} + 2H^+ + 2e^- \quad (10)$$

Table 1 shows the active units of AChE per electrode and their corresponding oxidation current responses in 0.1 M PBS (pH 9.0) solution containing 10 mM ATCh at a scan rate of 50 mV/s. It is evidently revealed that different clay/AuNPs resulted in varied AChE loadings and, correspondingly, the current responses,[27] as shown in Table 1. Figure S5 shows the effect of the scan rate on the oxidation peak currents of SPE/clay/AuNPs/AChE/CS. The linear relations of the peak currents with the square root of the scan rates (insets of Figure S5) suggest that the overall process was a typical diffusion control,[42] as was also detected in the case of $[Fe(CN)_6]^{3-/4-}$.

To optimize the performance of SPE/clay/AuNPs/AChE/CS biosensors, experimental conditions, including the pH of buffer solutions and the concentration of ATCh solutions, were investigated by the amperometric method. Figure S6 confirms that the current responses of all the SPE/clay/AuNPs/AChE/CS biosensors increased with increasing solution pH and peaked at pH 9.0. The pH of the buffer solutions certainly affected the charge property of modified-electrode materials and hence the activity of the immobilized AChE. Similar to the reported 8.0−9.0 optimum pH for soluble AChE,[43,44] the suitable solution pH for immobilized AChE in our cases was 9.0. Therefore, solutions at pH 9.0 were adopted in all of the following experiments.

The optimal ATCh concentration for pesticide detection was determined using an amperometric technique on SPE/clay/AuNPs/AChE/CS biosensors. The results displayed in Figure S7 demonstrate that the current response increases with ATCh concentration over the range from 0.5 to 10 mM where it reaches the plateau in most cases, except for the SPE/Kaol/AuNPs/AChE/CS biosensor. SPE/Kaol/AuNPs/AChE/CS provides the highest current response at 15 mM ATCh. The highest negatively charged Kaol/AuNPs,[27] which provided the strongest barrier to ATCh diffusion, was likely the cause of this difference. Thus, solutions with 10 mM ATCh were applied for the SPE/Mt/AuNPs/AChE/CS, SPE/Bent/AuNPs/AChE/CS, and SPE/Sep/AuNPs/AChE/CS biosensors, while 15 mM ATCh was used for the SPE/Kaol/AuNPs/AChE/CS biosensor.

3.4. Application of SPE/Clay/AuNPs/AChE/CS Biosensors for Pesticide Detection. *3.4.1. Pesticide Incubation Time.* Determination of pesticides (OPs and/or CMs) by AChE biosensors is achieved through the inhibition process. Incubating the enzyme in a solution with pesticides causes AChE inhibition by phosphorylation or carbamylation of the serine residue in the enzyme active site;[45,46] thus, pesticide determination can be completed following eq 4. Consequently, the effect of pesticide incubation time on the amperometric response toward the ATCh substrate was investigated separately in solutions with 200 ng/mL chlorpyrifos or 200 ng/mL carbaryl, as shown in Figure S8. With increases in the incubation period, the percentage of inhibition escalates almost

https://doi.org/10.1021/acsomega.2c03899
ACS Omega 2022, 7, 39848−39859

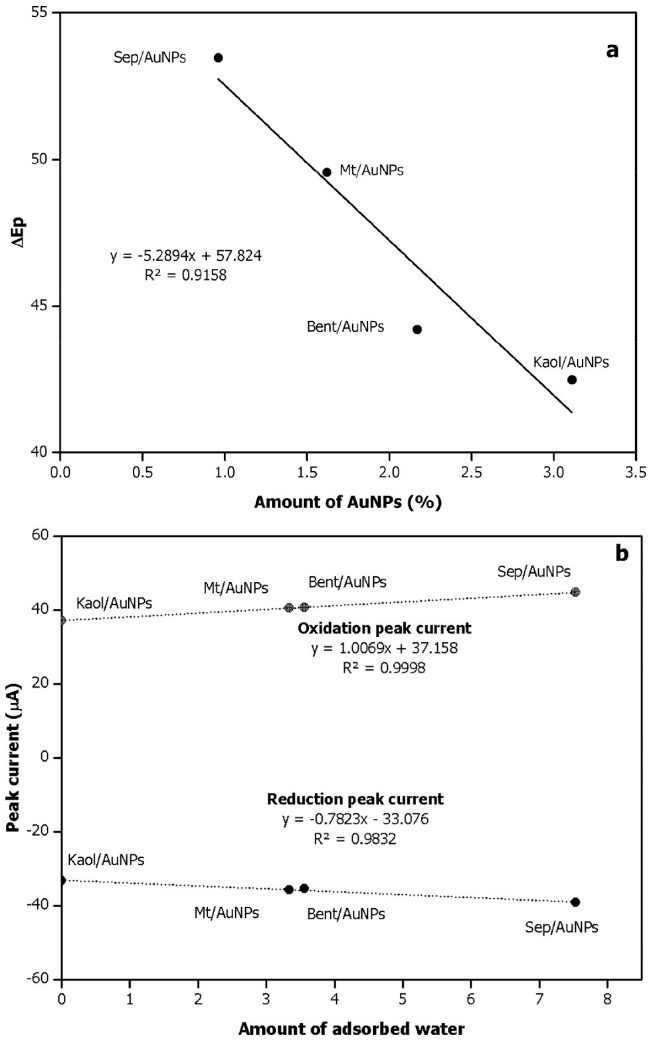

Figure 3. (a) Effects of the amounts of AuNPs on peak potential separation ΔE_p, and the (b) amounts of adsorbed water on peak currents of SPE/clay/AuNPs/CS in 0.1 M PBS (pH 9.0) containing 10 mM $[Fe(CN)_6]^{3-/4-}$ with 0.1 M KCl; scan rate 50 mV/s.

linearly with time before reaching a plateau at 10 min, indicating saturation of the serine active sites with pesticides.[4] Thus, an incubation time of 10 min was applied for all the following assays.

3.4.2. SPE/Clay/AuNPs/AChE/CS Biosensors for Analyses of Single and Mixed Pesticides. Sections 3.13.23.3 elaborates complicated effects of diverse characteristics of pristine clays on clay/AuNP syntheses and their applications as sensors. To further investigate the influences of these distinct modified-electrode materials on pesticide detection, different SPE/clay/AuNPs/AChE/CS biosensors were tested with chlorpyrifos, carbaryl, and their mixtures at equivalent concentrations. The calibration curves of the pesticides from the biosensors are shown in Figure 4. Under the optimal experimental conditions, two linear ranges are observed in all cases. It is worth noting that the inhibition percentage of the pesticide mixtures tends to lie between the two singular sources. Comparisons of the performance factors of the proposed biosensors are summarized in Table 2. The linear ranges of different biosensors in varied solutions are found suitable to the MRLs of the pesticides,[47,48] while the LODs which affect the pesticide discrimination capacity of the biosensors were statistically analyzed. The analyses were performed both in terms of different biosensors for the same pesticide solution (designated as superscripted a, b, c, and d) and the same biosensor for different solutions (as superscripted 1, 2, and 3). The results indicate that sensitivities (or LODs) of contrasting electrodes toward the same solution as well as the same sensor to varied solutions are statistically different. This is beneficial for the PCA, which will be demonstrated in the next section. Moreover, the LODs of the pesticide mixtures are mostly in between the boundaries of the two individual pesticides. Interestingly, the more hydrophobic the modified-electrode material, the more sensitive (the lower LODs) the detection of the specified pesticide(s), namely, chlorpyrifos,[27] carbaryl, or the mixture of the two pesticides. This is because pesticides are highly nonpolar. Thus, the clay/AuNPs with more hydrophobicity resulted in a higher pesticide concentration in the enzyme carrier and a higher diffusion rate of pesticide(s) to the enzyme matrix.[27,49] Therefore, greater enzyme inhibition was achieved. As shown in Table 2, the LODs for any specified pesticide(s) are in following order SPE/Kaol/AuNPs/AChE/CS < SPE/Mt/AuNPs/AChE/CS < SPE/Bent/AuNPs/AChE/CS < SPE/Sep/AuNPs/AChE/CS which corresponds to the hydrophobicity of the clay/AuNPs. Thus, the hydrophobic/hydrophilic nature of the modified-electrode materials, again, exhibited as one of the governing parameters for the sensor performances as already demonstrated for a highly polar solute, $[Fe(CN)_6]^{3-/4-}$. Surprisingly, the amounts of immobilized active AChE per electrode (Table 1) did not play a governing role in the biosensor sensitivity for pesticide detection, in contrast to what was reported elsewhere.[50] The reproducibility of SPE/clay/AuNPs/AChE/CS biosensors was evaluated under the optimum experimental conditions. The current response of each modified material is shown in Table S1. The reproducibility was presented by a relative standard deviation (R.S.D.) of the current response of each biosensor. The R.S.D. values of the current response (n = 10) were 3.77, 5.15, 5.67, and 7.46% for SPE/Kaol/AuNPs/AChE/CS, SPE/Mt/AuNPs/AChE/CS, SPE/Bent/AuNPs/AChE/CS, and SPE/Sep/AuNPs/AChE/CS biosensors, respectively.

Up to this point, we have established that the differences in physical and chemical characteristics of the selected pristine clays undoubtedly control the distinctive properties of the derived clay/AuNPs and their applications as modified-electrode materials in pesticide biosensors. Diverse amounts of AuNPs and AChE loadings as well as different hydrophobic/hydrophilic characters of the matrices were apparent among the studied clay/AuNPs. Nonetheless, all the proposed electrodes (SPE/clay/AuNPs/AChE/CS) displayed a diffusion-control process toward the ATCh substrate. Similar two linear ranges were, in addition, attained in all the tested biosensors for either a single or mixed pesticide determination. On the other hand, LODs of the determined pesticide(s) were revealed to correspond to the toxicity of the pesticides and hydrophobicity of the clay/AuNPs. That is the more toxic the pesticide and the more hydrophobic the modified-electrode material, the more sensitive the pesticide biosensor. The amounts of AChE loading were not found to influence the sensor sensitivity for pesticides but the current responses toward the ATCh substrate. Ultimately, we strongly anticipated that differentiation of pesticide types and concentration levels could be achieved through a combination of pesticide determinations utilizing diverse SPE/clay/AuNPs/AChE/CS

https://doi.org/10.1021/acsomega.2c03899
ACS Omega 2022, 7, 39848−39859

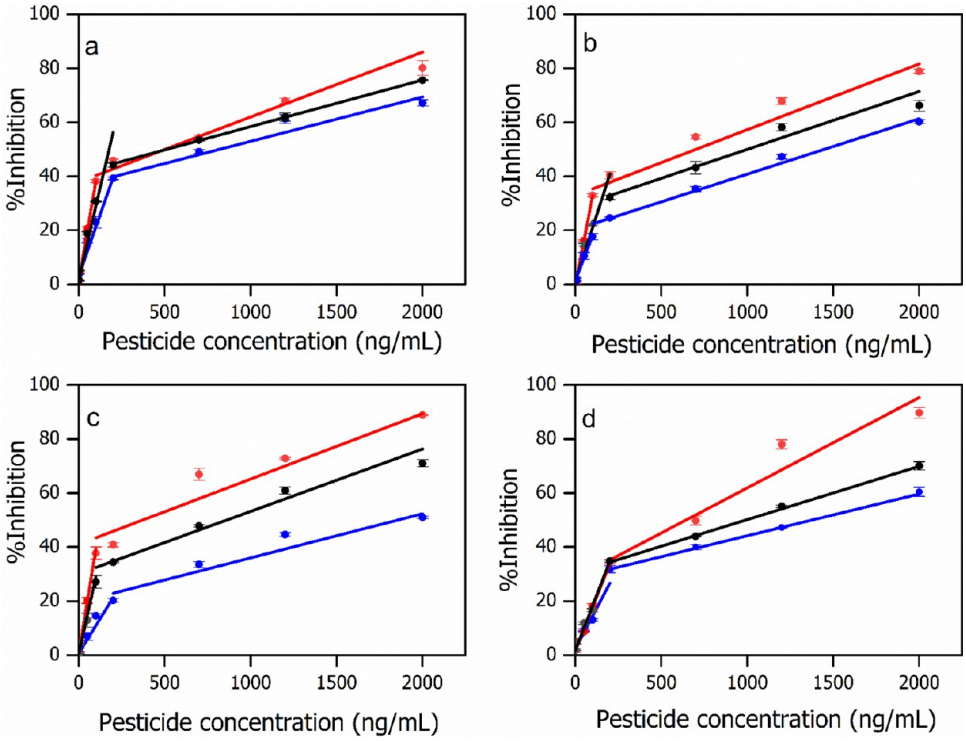

Figure 4. Calibration plots of chlorpyrifos (blue line), carbaryl (red line), and the mixture of chlorpyrifos and carbaryl (black line) by (a) SPE/Kaol/AuNPs/AChE/CS CS biosensor in 0.1 M PBS (pH 9.0) containing 15 mM ATCh, (b) SPE/Mt/AuNPs/AChE/CS, (c) SPE/Bent/AuNPs/AChE/CS, and (d) SPE/Sep/AuNPs/AChE/CS biosensors in 0.1 M PBS (pH 9.0) containing 10 mM ATCh.

Table 2. Performances of the SPE/Clay/AuNPs/AChE/CS Biosensor for Chlorpyrifos, Carbaryl, and a Mixture of Chlorpyrifos and Carbaryl[ab]

pesticide	sensor	linear range (ng/mL)	LOD (ng/mL)
chlorpyrifos	SPE/Kaol/AuNPs/AChE/CS	0.5−200, 200−2000	0.28 ± 0.01[a,1]
	SPE/Mt/AuNPs/AChE/CS	0.5−100, 100−2000	0.48 ± 0.04[b,1]
	SPE/Bent/AuNPs/AChE/CS	0.5−200, 200−2000	0.65 ± 0.04[c,1]
	SPE/Sep/AuNPs/AChE/CS	0.5−200, 200−2000	0.71 ± 0.04[d,1]
carbaryl	SPE/Kaol/AuNPs/AChE/CS	0.5−100, 100−2000	0.09 ± 0.01[a,2]
	SPE/Mt/AuNPs/AChE/CS	0.5−100, 100−2000	0.10 ± 0.01[b,2]
	SPE/Bent/AuNPs/AChE/CS	0.5−100, 100−2000	0.15 ± 0.01[c,2]
	SPE/Sep/AuNPs/AChE/CS	0.5−200, 200−2000	0.48 ± 0.05[d,2]
the mixture of chlorpyrifos and carbaryl	SPE/Kaol/AuNPs/AChE/CS	0.5−200, 200−2000	0.03 ± 0.01[a,3]
	SPE/Mt/AuNPs/AChE/CS	0.5−200, 200−2000	0.12 ± 0.02[b,3]
	SPE/Bent/AuNPs/AChE/CS	0.5−100, 100−2000	0.38 ± 0.03[c,3]
	SPE/Sep/AuNPs/AChE/CS	0.5−200, 200−2000	0.48 ± 0.03[d,2]

[a]Statistical analysis results show that values of the same letter (a, b, c, d) within the same column of each pesticide are not significantly different and vice versa for values of different letters within the same column of each pesticide. [b]Statistical analysis results show that values of the same letter (1, 2, 3) within the same sensor of each pesticide are not significantly different and vice versa for values of different letters within the same sensor of each pesticide.

biosensors and PCA, which will be demonstrated in the following section.

3.5. PCA Results of Synthetic Pesticide and Real Sample Solutions. To discriminate the pesticide types and concentration levels, PCA was employed to analyze the AChE inhibition data obtained from four different SPE/clay/AuNPs/AChE/CS biosensors. Figure 5 shows the PCA score plots of chlorpyrifos (a) and carbaryl (b). The first two principal components of the data variances are, respectively, 99.6 and 99.7% for chlorpyrifos and carbaryl. The high first principal component (PC1) value obtained (PC1 determined at 99.1 and 97.3% of the data variance for chlorpyrifos and carbaryl, respectively) indicates a good correlation between the data.[51] All the PCA plots indicate clusters of the triplicate results at different pesticide concentrations. Thus, PC1 presumably reflects the concentration of pesticides. In other words, the more positive the location of the data on PC1, the higher the pesticide concentration. Furthermore, Figure 5c shows a single PCA plot of both the inhibition data obtained separately from chlorpyrifos and carbaryl. Again, the obtained high total contribution variance of 98.4% indicates a good data correlation. Interestingly, two distinct regions of the data on PC2 are realized specifically for chlorpyrifos (negative PC2) and carbaryl (positive PC2). The ability to discriminate chlorpyrifos from carbaryl was certainly due to the different and unique inhibition responses (sensitivity) of each SPE/

https://doi.org/10.1021/acsomega.2c03899
ACS Omega 2022, 7, 39848−39859

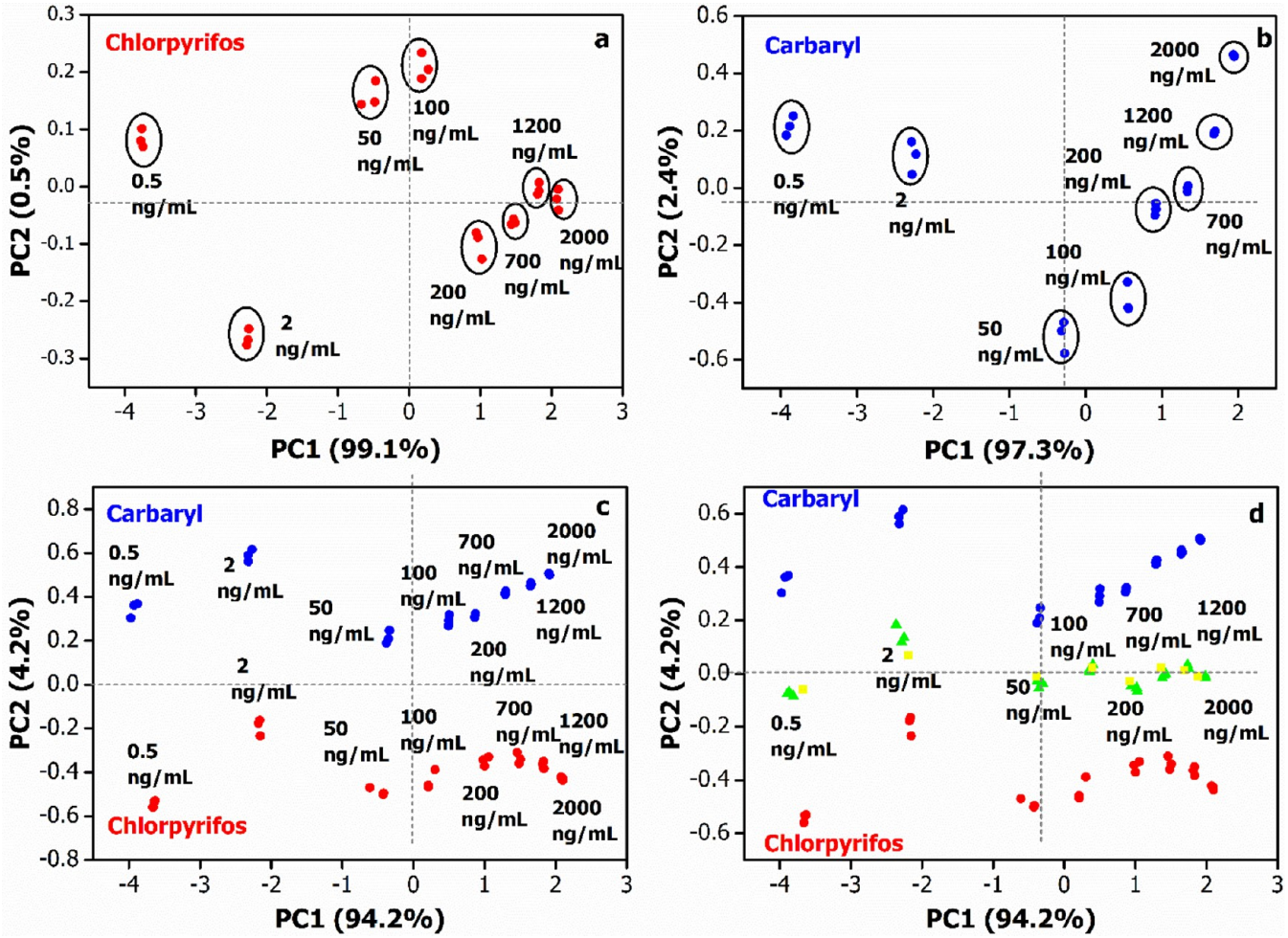

Figure 5. PCA score plots of (a) chlorpyrifos, (b) carbaryl, (c) singular chlorpyrifos and carbaryl, and (d) mixture of chlorpyrifos and carbaryl (equivalent concentration) by four different electrodes, namely, SPE/Kaol/AuNPs/AChE/CS, SPE/Mt/AuNPs/AChE/CS, SPE/Bent/AuNPs/AChE/CS, and SPE/Sep/AuNPs/AChE/CS biosensors.

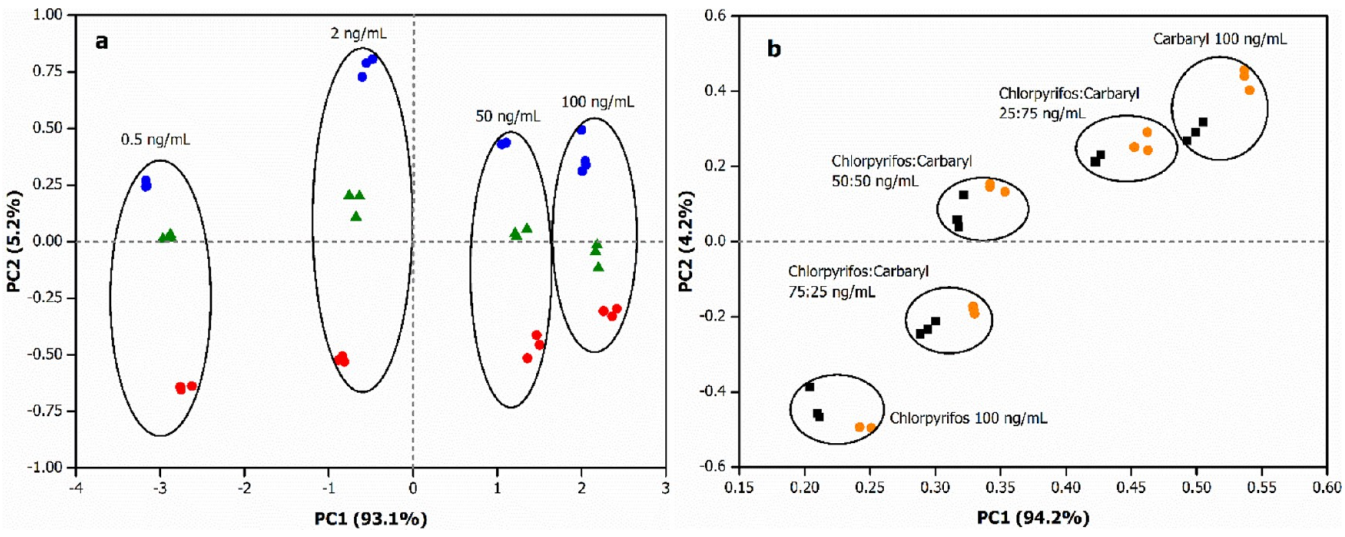

Figure 6. (a) PCA score plots of chlorpyrifos (red dot), carbaryl (blue dot), and a mixture of chlorpyrifos and carbaryl at equivalent concentrations (green dot) in the carrot sample, (b) PCA score plots of a mixture of chlorpyrifos and carbaryl at different concentration ratios in synthetic pesticide solutions (black dot) and carrot samples (orange dot) using SPE/Kaol/AuNPs/AChE/CS, SPE/Mt/AuNPs/AChE/CS, SPE/Bent/AuNPs/AChE/CS, and SPE/Sep/AuNPs/AChE/CS sensors.

clay/AuNPs/AChE/CS biosensor for each pesticide. Moreover, PC2 most likely designates the toxicity of pesticides where the higher PC2 value represents higher pesticide toxicity. On the other hand, PC1 once again suggests

https://doi.org/10.1021/acsomega.2c03899
ACS Omega 2022, 7, 39848−39859

concentration levels of the pesticides. Figure 5d exhibits a PCA plot of the inhibition data from individual chlorpyrifos (red dot), carbaryl (blue dot), and the binary mixture of chlorpyrifos and carbaryl (green dot) and the prediction of the mixture (yellow dot). The results obtained by predicting PCA are located around the experimental values of the mixture, which proves the accuracy of the prediction. No superposition of the distinct pesticide samples is observed. Similar to Figure 5c, PC1 and PC2 correspondingly represent the levels of pesticide concentration and toxicity. As a result, data from mixed pesticide solutions lie approximately in the middle of the boundaries of the two singular pesticides. The proposed biosensor system demonstrates the capacity to discriminate chlorpyrifos and carbaryl in the mixtures ranging from the very low of 0.5 ng/mL (ppb) to the high concentration of 2000 ng/mL, comparable to/or better than previous reports on other pesticides.[21−24]

To assess the capability of the SPE/clay/AuNPs/AChE/CS biosensors in differentiating chlorpyrifos and carbaryl in real samples, we performed the pesticide detection in carrot samples (see Figure S9) both at different concentration levels (at equivalent ratios) and varied mixture ratios (at the same total pesticide concentration). The PCA results are shown in Figure 6a,b. Chlorpyrifos, carbaryl, and a mixture of chlorpyrifos and carbaryl (equivalent concentration) in carrot solutions were measured in the range of 0.5−100 ng/mL (Figure 6a). The proposed biosensors were able to discriminate all the solutions by PCA, yielding a PCA without any superposition of the distinct groups of samples, while good proximity of the samples having the same pesticide concentrations could be observed. Figure 6a presents the score plot in the first two principal components of the data variances of chlorpyrifos, carbaryl, and their mixture in the carrot sample. In total, 98.2% of the variance has been retained from two principal components. PC1 contributed 93.1% of the variance, while PC2 contributed 5.2%. Clearly, the separation of pesticide types is visualized in the PC2 coordinates, while the separation of pesticide concentration is revealed in the PC1 coordinates.

Figure 6b shows a PCA plot of the inhibition data from the mixtures of chlorpyrifos and carbaryl at different concentration ratios. The black dots represent the results of synthetic pesticide, while the green dots show the results from the real sample. The PCA of the mixture is located without superposition of the different concentration ratios and tended to lie between the two singular pesticides. The PCA of the mixture in the real sample is not superimposed with the synthetic solutions; however, different mixture ratios can be clearly identified likewise.

4. CONCLUSIONS

This work ultimately demonstrates the successful utilization of the four different biosensors together with PCA for discrimination of chlorpyrifos and carbaryl and their concentration levels both in synthetic pesticide solution and real samples. The diverse biosensors were all fabricated based on the low-cost and simple clay/AuNPs of distinct characteristics for immobilization of the sole AChE. The four clay base minerals employed were Kaol, Mt, Bent, and Sep, whose characteristics resulted in different physical morphologies, AuNPs sizes and loadings, matrix hydrophobicity, and active AChE loading per electrode. These disparate characteristics of the clay/AuNPs were critical since they resulted in the biosensors with different sensitivities for each pesticide. Therefore, the distinction of the pesticide types and concentration levels was achieved using solely AChE as the catalyst. It was highlighted that incorporated AuNPs and the hydrophobic/hydrophilic character of the clay/AuNPs composites played governing roles in the biosensor performances. While the AuNPs resulted in tremendous enhancement of the electron transfer, the hydrophobicity of the clay/AuNPs affected the accumulation and diffusion rate of ATCh and pesticides to and/or within the modified electrodes. All the tested biosensors were disclosed to exhibit a diffusion-controlled mechanism toward the ATCh substrate.

Under the optimum conditions for pesticide determination, the four clay/AuNPs/AChE-based biosensors were tested in the synthetic and carrot solutions of chlorpyrifos, carbaryl, and their mixtures. It was disclosed that the higher enzyme inhibition and the more hydrophobic the modified-electrode material, the more sensitive the pesticide biosensor. PCA of the vastly obtained results from the four disparate biosensors demonstrated the successful discrimination of the pesticide types and their concentration levels as well as the different concentration ratios of binary mixtures. Therefore, it could be summarized that the hydrophobic/hydrophilic character of the material plays a major role indiscriminating the pesticide by the proposed single-enzyme sensor system. To the best of our knowledge, this work establishes the employment of the cheap and simple yet diverse characteristics of the different clay/AuNPs as modified-electrode materials for AChE biosensors for the discrimination of pesticide types and concentration levels both in the synthetic and real solutions. The mixed pesticides could be identified at an especially low total concentration of 0.5 ng/mL in real samples.

■ ASSOCIATED CONTENT

Supporting Information

The Supporting Information is available free of charge at https://pubs.acs.org/doi/10.1021/acsomega.2c03899.

XPS and TGA observed for the modified material (clay/AuNPs); the cyclic voltammetry results of SPE/clay/CS and SPE/clay/AuNPs/CS observed at various scan rates in 10 mM $Fe(CN_6)^{3-/4-}$; the cyclic voltammetry results of SPE/clay/AuNPs/AChE/CS observed at various scan rates in 10 mM ATCh; the optimum pH and ATCh concentration of the SPE/clay/AuNPs/AChE/CS biosensor obtained from the amperometric method; the incubation time of chlorpyrifos and carbaryl observed; effect of concentration ratios of chlorpyrifos and carbaryl on the SPE/clay/AuNPs/AChE/CS biosensor (PDF)

■ AUTHOR INFORMATION

Corresponding Author

Thanawee Chodjarusawad − *Department of Physics, Faculty of Science, Burapha University, Chonburi 20131, Thailand;* orcid.org/0000-0002-5909-5484; Phone: (+66) 3810 3143; Email: thitikor@buu.ac.th

Authors

Angkana Phongphut − *Department of Chemical Engineering, Faculty of Engineering, Chulalongkorn University, Bangkok 10330, Thailand*

Bralee Chayasombat − *National Metal and Materials Technology Center, Pathumthani 12120, Thailand*

https://doi.org/10.1021/acsomega.2c03899
ACS Omega 2022, 7, 39848−39859

Anthony E. G. Cass − *Department of Chemistry, Imperial College London, London W12 0NZ, U.K.;* orcid.org/0000-0001-8881-4786

Muenduen Phisalaphong − *Department of Chemical Engineering, Faculty of Engineering, Chulalongkorn University, Bangkok 10330, Thailand*

Seeroong Prichanont − *Department of Chemical Engineering, Faculty of Engineering, Chulalongkorn University, Bangkok 10330, Thailand*

Chanchana Thanachayanont − *National Metal and Materials Technology Center, Pathumthani 12120, Thailand*

Complete contact information is available at: https://pubs.acs.org/10.1021/acsomega.2c03899

Notes

The authors declare no competing financial interest.

■ ACKNOWLEDGMENTS

This work was supported by The Royal Golden Jubilee (RGJ) PhD Program, (PhD/0235/2558), Newton Fund-TRF PhD Programs − Placement for Scholars 2017/18, and Thailand National and Materials Technology Center.

■ REFERENCES

(1) da Silva, W.; Brett, C. M. A. Novel biosensor for acetylcholine based on acetylcholinesterase/poly(neutral red) − Deep eutectic solvent/Fe2O3 nanoparticle modified electrode. *J. Electroanal. Chem.* **2020**, *872*, No. 114050.

(2) Montali, L.; Calabretta, M. M.; Lopreside, A.; D'Elia, M.; Guardigli, M.; Michelini, E. Multienzyme chemiluminescent foldable biosensor for on-site detection of acetylcholinesterase inhibitors. *Biosens. Bioelectron.* **2020**, *162*, No. 112232.

(3) Shrestha, S.; Parks, C. G.; Umbach, D. M.; Richards-Barber, M.; Hofmann, J. N.; Chen, H.; Blair, A.; Beane Freeman, L. E.; Sandler, E. P. Pesticide use and incident Parkinson's disease in a cohort of farmers and their spouses. *Environ. Res.* **2020**, *191*, No. 110186.

(4) Lang, Q.; Han, L.; Hou, C.; Wang, F.; Liu, A. A sensitive acetylcholinesterase biosensor based on gold nanorods modified electrode for detection of organophosphate pesticide. *Talanta* **2016**, *156−157*, 34−41.

(5) Patel, H.; Rawtani, D.; Agrawal, Y. K. A newly emerging trend of chitosan-based sensing platform for the organophosphate pesticide detection using Acetylcholinesterase- a review. *Trends Food Sci. Technol.* **2019**, *85*, 78−91.

(6) Valdés-Ramírez, G.; Gutiérrez, M.; del Valle, M.; Ramírez-Silva, M. T.; Fournier, D.; Marty, J. L. Automated resolution of dichlorvos and methylparaoxon pesticide mixtures employing a Flow Injection system with an inhibition electronic tongue. *Biosens. Bioelectron.* **2009**, *24*, 1103−1108.

(7) Verma, N.; Bhardwaj, A. Biosensor Technology for Pesticides—A review. *Appl. Biochem. Biotechnol.* **2015**, *175*, 3093−3119.

(8) Zhao, F.; Wu, J.; Ying, Y.; She, Y.; Wang, J.; Ping, J. Carbon nanomaterial-enabled pesticide biosensors: Design strategy, biosensing mechanism, and practical application. *TrAC, Trends Anal. Chem.* **2018**, *106*, 62−83.

(9) Bilal, S.; Mudassir, H. M.; Fayyaz ur Rehman, M.; Nasir, M.; Jamil Sami, A.; Hayat, A. An insect acetylcholinesterase biosensor utilizing WO3/g-C3N4 nanocomposite modified pencil graphite electrode for phosmet detection in stored grains. *Food Chem.* **2021**, *346*, No. 128894.

(10) Liang, B.; Wang, G.; Yan, L.; Ren, H.; Feng, R.; Xiong, Z.; Liu, A. Functional cell surface displaying of acetylcholinesterase for spectrophotometric sensing organophosphate pesticide. *Sens. Actuators, B* **2019**, *279*, 483−489.

(11) Chu, S.; Huang, W.; Shen, F.; Li, T.; Li, S.; Xu, W.; Lv, C.; Luo, Q.; Liu, J. Graphene oxide-based colorimetric detection of organophosphorus pesticides via a multi-enzyme cascade reaction. *Nanoscale* **2020**, *12*, 5829−5833.

(12) Liang, B.; Han, L. Displaying of acetylcholinesterase mutants on surface of yeast for ultra-trace fluorescence detection of organophosphate pesticides with gold nanoclusters. *Biosens. Bioelectron.* **2020**, *148*, No. 111825.

(13) Wang, S.; Ye, Z.; Wang, X.; Xiao, L. Etching of Single-MnO2-Coated Gold Nanoparticles for the Colorimetric Detection of Organophosphorus Pesticides. *ACS Appl. Nano Mater.* **2019**, *2*, 6646−6654.

(14) Karnati, C.; Du, H.; Ji, H.-F.; Xu, X.; Lvov, Y.; Mulchandani, A.; Mulchandani, P.; Chen, W. Organophosphorus hydrolase multilayer modified microcantilevers for organophosphorus detection. *Biosens. Bioelectron.* **2007**, *22*, 2636−2642.

(15) Facure, M. H. M.; Mercante, L. A.; Mattoso, L. H. C.; Correa, D. S. Detection of trace levels of organophosphate pesticides using an electronic tongue based on graphene hybrid nanocomposites. *Talanta* **2017**, *167*, 59−66.

(16) Ni, Y.; Kokot, S. Does chemometrics enhance the performance of electroanalysis? *Anal. Chim. Acta* **2008**, *626*, 130−146.

(17) Czolkos, I.; Dock, E.; Tønning, E.; Christensen, J.; Winther-Nielsen, M.; Carlsson, C.; Mojzíková, R.; Skládal, P.; Wollenberger, U.; Nørgaard, L.; Ruzgas, T.; Emnéus, J. Prediction of wastewater quality using amperometric bioelectronic tongues. *Biosens. Bioelectron.* **2016**, *75*, 375−382.

(18) Solná, R.; Dock, E.; Christenson, A.; Winther-Nielsen, M.; Carlsson, C.; Emnéus, J.; Ruzgas, T.; Skládal, P. Amperometric screen-printed biosensor arrays with co-immobilised oxidoreductases and cholinesterases. *Anal. Chim. Acta* **2005**, *528*, 9−19.

(19) Tønning, E.; Sapelnikova, S.; Christensen, J.; Carlsson, C.; Winther-Nielsen, M.; Dock, E.; Solna, R.; Skladal, P.; Nørgaard, L.; Ruzgas, T.; Emnéus, J. Chemometric exploration of an amperometric biosensor array for fast determination of wastewater quality. *Biosens. Bioelectron.* **2005**, *21*, 608−617.

(20) Qian, S.; Lin, H. Colorimetric Sensor Array for Detection and Identification of Organophosphorus and Carbamate Pesticides. *Anal. Chem.* **2015**, *87*, 5395−5400.

(21) Chen, L.; Tian, X.; Li, Y.; Lu, L.; Nie, Y.; Wang, Y. Broad-spectrum pesticide screening by multiple cholinesterases and thiocholine sensors assembled high-throughput optical array system. *J. Hazard. Mater.* **2021**, *402*, No. 123830.

(22) Madianos, L.; Skotadis, E.; Patsiouras, L.; Filippidou, M. K.; Chatzandroulis, S.; Tsoukalas, D. Nanoparticle based gas-sensing array for pesticide detection. *J. Environ. Chem. Eng.* **2018**, *6*, 6641−6646.

(23) He, Y.; Xu, B.; Li, W.; Yu, H. Silver Nanoparticle-Based Chemiluminescent Sensor Array for Pesticide Discrimination. *J. Agric. Food Chem.* **2015**, *63*, 2930−2934.

(24) Bordbar, M. M.; Nguyen, T. A.; Arduini, F.; Bagheri, H. A paper-based colorimetric sensor array for discrimination and simultaneous determination of organophosphate and carbamate pesticides in tap water, apple juice, and rice. *Microchim. Acta* **2020**, *187*, 621−621.

(25) An, N.; Zhou, C. H.; Zhuang, X. Y.; Tong, D. S.; Yu, W. H. Immobilization of enzymes on clay minerals for biocatalysts and biosensors. *Appl. Clay Sci.* **2015**, *114*, 283−296.

(26) Chang, M. Y.; Kao, H. C.; Juang, R. S. Thermal inactivation and reactivity of β-glucosidase immobilized on chitosan−clay composite. *Int. J. Biol. Macromol.* **2008**, *43*, 48−53.

(27) Phongphut, A.; Chayasombat, B.; Cass, A. E. G.; Sirisuk, A.; Phisalaphong, M.; Prichanont, S.; Thanachayanont, C. Clay/au nanoparticle composites as acetylcholinesterase carriers and modified-electrode materials: A comparative study. *Appl. Clay Sci.* **2020**, *194*, No. 105704.

(28) Sarkar, B., Singh, M., Mandal, S., Churchman, G.J., Bolan, N.S.Chapter 3 - Clay Minerals—Organic Matter Interactions in Relation to Carbon Stabilization in Soils. In *The Future of Soil Carbon*; Garcia, C., Nannipieri, P, Hernandez, T, Eds.; Academic Press, 2018; pp 71−86.

(29) Yao, M.; Dong, Y.; Feng, X.; Hu, X.; Jia, A.; Xie, G.; Hu, G.; Lu, J.; Luo, M.; Fan, M. The effect of post-processing conditions on aminosilane functionalizaiton of mesocellular silica foam for post-combustion CO2 capture. *Fuel* **2014**, *123*, 66−72.
(30) Ellman, G. L.; Courtney, K. D.; Andres, V.; Featherstone, R. M. A new and rapid colorimetric determination of acetylcholinesterase activity. *Biochem. Pharmacol.* **1961**, *7*, 88−95.
(31) Houngkamhang, N.; Phasukkit, P. Portable Deep Learning-Driven Ion-Sensitive Field-Effect Transistor Scheme for Measurement of Carbaryl Pesticide. *Sensors* **2022**, *22*, 3543.
(32) Li, C.; Dong, X.; Zhu, N.; Zhang, X.; Yang, S.; Sun, Z.; Liu, Y.; Zheng, S.; Dionysiou, D. D. Rational design of efficient visible-light driven photocatalyst through 0D/2D structural assembly: Natural kaolinite supported monodispersed TiO2 with carbon regulation. *Chem. Eng. J.* **2020**, *396*, No. 125311.
(33) Zhang, S.; Liu, Q.; Yang, Y.; Wang, D.; He, J.; Sun, L. Preparation, morphology, and structure of kaolinites with various aspect ratios. *Appl. Clay Sci.* **2017**, *147*, 117−122.
(34) Sundrarajan, M.; Bama, K.; Selvanathan, G.; Ramesh Prabhu, M. Ionic liquid-mediated: Enhanced surface morphology of silver/manganese oxide/bentonite nanocomposite for improved biological activities. *J. Mol. Liq.* **2018**, *249*, 1020−1032.
(35) Oliveira, A. S.; Alcântara, A. C. S.; Pergher, S. B. C. Bionanocomposite systems based on montmorillonite and biopolymers for the controlled release of olanzapine. *Mater. Sci. Eng., C* **2017**, *75*, 1250−1258.
(36) Chen, S.; Yan, X.; Liu, W.; Qiao, R.; Chen, S.; Luo, H.; Zhang, D. Polymer-based dielectric nanocomposites with high energy density via using natural sepiolite nanofibers. *Chem. Eng. J.* **2020**, *401*, No. 126095.
(37) Zhou, F.; Yan, C.; Wang, H.; Zhou, S.; Komarneni, S. Sepiolite-TiO2 nanocomposites for photocatalysis: Synthesis by microwave hydrothermal treatment versus calcination. *Appl. Clay Sci.* **2017**, *146*, 246−253.
(38) Wang, S.; Rogachev, A. A.; Yarmolenko, M. A.; Rogachev, A. V.; Xiaohong, J.; Gaur, M. S.; Luchnikov, P. A.; Galtseva, O. V.; Chizhik, S. A. Structure and properties of polyaniline nanocomposite coatings containing gold nanoparticles formed by low-energy electron beam deposition. *Appl. Surf. Sci.* **2018**, *428*, 1070−1078.
(39) Maghear, A.*Development of new types of composite electrodes based on natural clays and their analytical applications*, 2013.
(40) Kumari, R.; Opoku, F.; Osikoya, A. O.; Anku, W. W.; Shukla, S. K.; Govender, P. P. Hierarchically assembled two-dimensional goldboron nitride-tungsten disulphide nanohybrid interface system for electrobiocatalytic applications. *Mater. Chem. Phys.* **2019**, *226*, 129−140.
(41) Cui, H. F.; Wu, W. W.; Li, M. M.; Song, X.; Lv, Y.; Zhang, T. T. A highly stable acetylcholinesterase biosensor based on chitosan-TiO2-graphene nanocomposites for detection of organophosphate pesticides. *Biosens. Bioelectron.* **2018**, *99*, 223−229.
(42) Kumar, T. H. V.; Sundramoorthy, A. K. Electrochemical biosensor for methyl parathion based on single-walled carbon nanotube/glutaraldehyde crosslinked acetylcholinesterase-wrapped bovine serum albumin nanocomposites. *Anal. Chim. Acta* **2019**, *1074*, 131−141.
(43) Eisenthal, R., Danson, M.J.*Enzyme assays: a practical approach*; Oxford University Press: Oxford, U.K., 2002; p 302
(44) Xue, G.; Yue, Z.; Bing, Z.; Yiwei, T.; Xiuying, L.; Jianrong, L. Highly-sensitive organophosphorus pesticide biosensors based on CdTe quantum dots and bi-enzyme immobilized eggshell membranes. *Analyst* **2016**, *141*, 1105−1111.
(45) Ma, L.; Zhou, L.; He, Y.; Wang, L.; Huang, Z.; Jiang, Y.; Gao, J. Hierarchical nanocomposites with an N-doped carbon shell and bimetal core: Novel enzyme nanocarriers for electrochemical pesticide detection. *Biosens. Bioelectron.* **2018**, *121*, 166−173.
(46) Van Dyk, J. S.; Pletschke, B. Review on the use of enzymes for the detection of organochlorine, organophosphate and carbamate pesticides in the environment. *Chemosphere* **2011**, *82*, 291−307.
(47) Sukanya, S.*Thai FDA Revises Pesticide Residue Standards and MRLs in Food*. In: Health MoP, editor, 2017.
(48) Laohaudomchok, W.; Nankongnab, N.; Siriruttanapruk, S.; Klaimala, P.; Lianchamroon, W.; Ousap, P.; Jatiket, M.; Kajitvichyanukul, P.; Kitana, N.; Siriwong, W.; Hemachudhah, T.; Satayavivad, J.; Robson, M.; Jaacks, L.; Barr, D. B.; Kongtip, P.; Woskie, S. Pesticide use in Thailand: Current situation, health risks, and gaps in research and policy. *Hum. Ecol. Risk Assess.* **2021**, *27*, 1147−1169.
(49) Allen, T. W.; Kuyucak, S.; Chung, S. H. The effect of hydrophobic and hydrophilic channel walls on the structure and diffusion of water and ions. *J. Chem. Phys.* **1999**, *111*, 7985−7999.
(50) Rajangam, B.; Daniel, D. K.; Krastanov, A. I. Progress in enzyme inhibition based detection of pesticides. *Eng. Life Sci.* **2018**, *18*, 4−19.
(51) de Queiroz, D. P.; Florentino, A. O.; Bruno, J. C.; da Silva, J. H. D.; Riul, A.; Giacometti, J. A. The use of an e-tongue for discriminating ethanol/water mixtures and determination of their water content. *Sens. Actuators, B* **2016**, *230*, 566−570.

https://doi.org/10.1021/acsomega.2c03899
ACS Omega 2022, 7, 39848−39859